The 11q-Gain/Loss Aberration Occurs Recurrently in *MYC*-Negative Burkitt-like Lymphoma With 11q Aberration, as Well as *MYC*-Positive Burkitt Lymphoma and *MYC*-Positive High-Grade B-Cell Lymphoma, NOS

Beata Grygalewicz, PhD,[1] Renata Woroniecka, PhD,[1] Grzegorz Rymkiewicz, MD, PhD,[1,2] Jolanta Rygier, MS,[1] Klaudia Borkowska, MS,[1] Aleksandra Kotyl, MS,[1] Katarzyna Blachnio, MS,[2] Zbigniew Bystydzienski, PhD,[2] Beata Nowakowska, PhD,[3] and Barbara Pienkowska-Grela, PhD[1]

From the [1]Cytogenetic Laboratory, Maria Sklodowska-Curie Institute Oncology Center, Warsaw, Poland; [2]Flow Cytometry Laboratory, Pathology and Laboratory Diagnostics Department, Maria Sklodowska-Curie Institute Oncology Center, Warsaw, Poland; and [3]Department of Medical Genetics, Mother and Child Institute, Warsaw, Poland.

Key Words: 11q-gain/loss; Burkitt-like lymphoma with 11q aberration; *KMT2A*; *MYC*; High-grade B-cell lymphoma

Am J Clin Pathol January 2018;149:17-28

DOI: 10.1093/AJCP/AQX139

ABSTRACT

Objectives: *The latest revision of lymphoma's World Health Organization classification describes the new provisional entity "Burkitt-like lymphoma with 11q aberration" (BLL, 11q) as lacking* MYC *rearrangement, but harboring the specific11q-gain/loss aberration. We report genetic characteristics of 11 lymphoma cases with this aberration.*

Methods: *Classical cytogenetics, fluorescence in situ hybridization (FISH), and single nucleotide polymorphism/array comparative genomic hybridization.*

Results: *The 11q aberrations were described as duplication, inversion, and deletion. Array comparative genomic hybridization showed two types of duplication: bigger than 50 megabase pairs (Mbp) and smaller than 20 Mbp, which were associated with bulky tumor larger than 20 cm and amplification of the 11q23.3 region, including* KMT2A. *Six cases revealed a normal FISH status of* MYC *and were diagnosed as BLL,11q. Five cases showed* MYC *rearrangement and were diagnosed as Burkitt lymphoma (BL) or high-grade B-cell lymphoma, not otherwise specified (HGBL, NOS).*

Conclusions: *The 11q-gain/loss is not specific for BLL, 11q, but occurs recurrently in* MYC*-positive BL and* MYC*-positive HGBL.*

Recurrent occurrence of duplication of 11q (dup(11q)) in four *MYC*-negative Burkitt lymphoma (BL) cases was initially described by Pienkowska-Grela et al.[1] Subsequent study of Salaverria et al[2] performed on 12 BL and Burkitt-like lymphoma cases (BLL) and two cell lines using high-resolution array-based comparative genomic hybridization (aCGH) showed that duplication/gain of 11q in these cases is constantly associated with loss of the terminal region of 11q, and the aberration was described as 11q-gain/loss. The authors postulated that 11q-gain/loss is specific for *MYC*-negative aggressive B-cell lymphomas resembling BL. Interestingly, this aberration was also found in three patients with posttransplant molecular BL signature without *MYC* rearrangement reported by Ferreiro et al.[3] aCGH studies allowed to define the minimal gained region at 11q23.3 (size 3.4 megabase pairs [Mbp]) and the minimal lost region at 11q24.1qter (size 7.4 Mbp).[2,3] Importantly, one case with a biallelic deletion of 1.5 Mbp at 11q24.3 was reported by Salaverria et al.[2] Coincidence of gain and loss of 11q suggests a simultaneous upregulation of oncogenes and downregulation of tumor suppressor gene(s), likely located at 11q23 and 11q24-qter, respectively. The candidate oncogene is the commonly upregulated *PAFAH1B2* gene, while two genes—*FLI1* and *ETS1*—located in the region of biallelic deletion and respectively downregulated and mutated, were postulated as candidate tumor suppressor genes

affected by this aberration.[2] The study of Ferreiro et al[3] detected overexpression of *USP2*, *CBL*, and *PAFAH1B2* located in the gained 11q23.3 region and simultaneous downregulation of *TBRG1*, *EI24*, and *ETS1* mapped in the lost 11q24q25 region.

On the basis of these discoveries, the 2016 revision of World Health Organization (WHO) classification of lymphoid neoplasms recognized a new provisional entity designated as "Burkitt-like lymphoma with 11q aberration" (BLL,11q).[4] This entity comprises B-cell lymphomas resembling BL morphologically, phenotypically, and by gene and microRNA expression profiling,[2,3,5] but lacking *MYC* rearrangement. Instead, they harbor 11q-gain/loss aberration. Notably, compared to classical BL, these lymphomas have more complex karyotypes.

Although 11q-gain/loss has been incorporated in the panel of diagnostically important genetic changes in lymphomas, number of cases harboring this aberration is very limited. Recently, Havelange et al[6] published four cases of *MYC*-positive high-grade B-cell lymphomas, not otherwise specified (HGBL, NOS) categories with 11q aberrations, including one case with 11q-gain/loss, suggesting that 11q aberration might not be specific for this new entity of mature B-cell lymphoma.

Here we present detailed cytogenetic characterization of 11q-gain/loss in 11 new lymphoma cases—six *MYC*-negative and five *MYC*-positive—showing features of typical, BLL,11q, BL, as well as HGBL, NOS.

Materials and Methods

Patients

The cases were selected from approximately 2,000 B-cell non-Hodgkin lymphoma (B-NHL) cases diagnosed routinely by classical cytogenetics (CC) in our hospital between 2000 and 2016. The diagnosis of BL, BLL,11q, and HGBL, NOS, was established according to the 2016 revision of the WHO lymphoma classification based on histopathologic/immunohistochemical examination (HP/IHC), with flow-cytometry analysis (FCM), CC, and fluorescence in situ hybridization (FISH). The inclusion criteria used for selecting cases comprised simple or low complex karyotype with recurrent 11q aberrations and HP/IHC features consistent with BL but also including B-cell lymphoma, unclassifiable (BCLU), with features intermediate between diffuse large B-cell lymphoma and BL morphology.[4] Immunohistochemistry was applied if necessary for each monoclonal antibody (MoAb) against: CD20, CD10, BCL6, BCL2, MYC, MUM1, CD43, CD44, Ki-67, CD3, and CD5 (Dako, Glostrum, Denmark; Novocastra Leica Microsystems, Berlin, Germany). An optimum panel of antihuman MoAbs used for the FCM analysis to evaluate B-NHLs, included CD (3/4/5/8/10/11c/16 + 56/19/20/22/23/25/38/43/44/45/52/56/62L/71/79β/81/200), FMC7/HLA-DR/BCL2/BCL6, and antibodies against light/heavy chains (κ/λ/IgD/IgM/IgG/IgA) (Becton Dickinson, Biosciences, San Jose, CA; AbD Serotec, Kidlington, UK; Invitrogen, Frederick, MD).

Classical Cytogenetics

Material for cytogenetic analysis was obtained from the involved lymphatic tissue by the fine needle aspiration biopsy (FNAB) or ultrasound-guided FNAB. Karyotype analysis followed standard protocols. Chromosomes were G/C-banded using Wright stain. At least eight metaphases per case were analyzed, using microscope Axioskop2 (Carl Zeiss, Jena, Germany) and IKAROS Imaging System (MetaSystems, Altlussheim, Germany). Karyotypes were classified according to the International System for Human Cytogenetic Nomenclature.[7]

FISH

FISH analysis was performed on cytogenetic specimens. FISH probes included MYC BAP, BCL2 BAP, BCL6 BAP, CCND1 BAP, MLL BAP, LSI ATM, TelVision 11q (D11S1037), and CEP11 (Vysis Abbott Molecular, Downers, Grove, IL). The procedures were applied according to the manufacturer's protocol. Slides were analyzed using an epifluorescence microscope Axioskop2 and documented by ISIS Imaging System (MetaSystems). In all cases at least 100 nuclei were scored, and presence of inversion was confirmed on chromosome spreads.

Single Nucleotide Polymorphism (SNP)/aCGH Protocol

DNA was extracted from fresh biopsy material or cytogenetic fixed-cell suspension by QIAmp DNA Blood Mini Kit (Qiagen, Valencia, CA) according to the manufacturer's recommendation. DNA of patient 10 was isolated from paraffin sections using DNA Sample Preparation Kit (Roche, Basel, Switzerland). The reference DNA was used from two pools (male and female) from normal individuals and run as a same-sex control. The control DNA for patient 10 was isolated from paraffin sections of normal lymph node. For SNP/aCGH analysis, CytoSure Haematological Cancer and SNP Array (8x60k) (Oxford Gene Technology [OGT], Yarnton, UK) was used. Total genomic DNA of 600 ng was processed in accordance with the manufacturer's protocol. Each patient and reference DNA was labeled with Cy3 and Cy5 dyes, respectively. Purification of labeled products, hybridization, and postwash of the array were carried out

DOI: 10.1093/AJCP/AQX139

according to OGT's recommendation. Array slides were scanned with Agilent G2565CA scanner, and images were quantified using Agilent Feature Extraction Software (version 10.7.3.1) (Agilent, Santa Clara, CA, USA).

SNP/aCGH Analysis

Array analysis was performed as described.[8] Briefly, CytoSure Interpret software, version 020022 (OGT), was used for analysis of array data. Deletion or duplication calls were made using the $\log_2$ ratio of each segment that has a minimum of four probes. Threshold factor for deletions was set as a $\log_2$ ratio of −0.6 that is less stringent than the theoretical $\log_2$ score of −1 (heterozygous deletion $\log_2(1/2) = -1$; no change in allele number $\log_2(2/2) = 0$; heterozygous duplication $\log_2(3/2) = 0.59$). The software uses the derivative log ratio (DLR) spread, which is used as a quality control check. This metric calculates probe-to-probe log ratio noise of an array and hence of the minimum log ratio difference required to make reliable amplification or deletion calls. A DLR of 0.08 to 0.19 is accepted, 0.20 to 0.29 is borderline, and 0.30 or greater is rejected. The DLR for all arrays was scored by this scale. The only two exceptions were patients 6 and 10 where the DLR was above 0.30. We decided to include these cases in the analysis because the array pattern of 11q changes was consistent with FISH results. The software calculated the total percentage homozygosity of each sample containing SNP data based on the method previously described by Sund et al.[9] The aCGH average resolution was 68 kilobase pairs (kbp), and the coverage of 11q was denser and equal to 46.6 kbp. The average SNP probes resolution was 30 Mbp. Gene positions and minimal regions of gain and loss in 11q were identified according to hg19 human genome build.

Statistical Analysis

Fisher's exact test, two-sided, was used to determine the significance of association of *KMT2A* multiplication with bigger duplication and bulky tumor (>20 cm). A *P* value less than .05 was considered statistically significant.

Results

Morphology, Immunohistochemical Characterization, and Final Diagnosis

Relevant clinical characteristics of the 11 reported cases are shown in Table 1. All patients were male and age 20 to 62 years (median age, 38 years). Morphologically, all cases showed a diffuse lymphoid infiltration, seven exhibited a classical starry-sky pattern typical for BL, while the other four slightly differed from BL features by the reduced number of macrophages and apoptotic bodies. In most tumors, the cell size was uniformly medium with round nuclei and a few small nucleoli typical for BL and BLL,11q. However, the lack of a jigsaw puzzle effect of cytoplasmic borders and a mild degree of irregular nuclear contours were noted in some tumors, especially in HGBL, NOS, with BCLU morphology. Based on HP, all 11 patients were morphologically diagnosed as BL or BCLU.[4] Examples of HP of four patients are demonstrated in Image 1. By IHC, all BLL,11q and BL were CD20+, CD10+, BCL6+, BCL2−, MUM1−, and MYC+ and showed a high proliferation rate. Among two cases of HGBL, NOS, with similar IHC, one had weak BCL2 expression (patient 10). By flow cytometry, BLL,11q immunophenotypically resembled *MYC*-positive BL and *MYC*-positive HGBL, NOS, with a few exceptions (G. Rymkiewicz, personal communication).

The final diagnosis of BLL,11q (six cases), BL (three cases), and HGBL, NOS (two cases), was made by the same hematopathologist according to the updated 2016 WHO classification, including HP (morphological) criteria and IHC examination, with CC and FISH analysis, along with clinical characteristics of all patients without lymphoma dissemination. Patients usually showed one enlarged tumor, or less frequently, a few enlarged tumors located nearby. None of the patients showed bone marrow or central nervous system involvement. Bulky tumor (>7 cm) was detected in six cases—among them, three patients presented large tumor with a diameter larger than 20 cm, mostly localized in the abdomen. In other cases, tumors were located in cervical, stomach, tonsil, intestine, and abdominal lymph nodes.

Classical Cytogenetics of 11q-Gain/Loss Cases

Karyotyping was successful in all 11 cases Table 2. Patient 4 showed a simple karyotype, while the remaining cases revealed complex karyotypes. All cases showed duplication of 11q, but size of duplication was variable Figure 1. The biggest duplicated region was located between 11q12.1 and 11q24.3 bands (patient 1) and the smallest duplicated region covered region between 11q22.3 and 11q24.1 (patient 5). In all cases but one (patient 6), one aberrant and one normal chromosome 11 were present. In patient 6, two or three different dup(11q) were detected. The first revealed simple dup(11)(q14q24), the second showed dup(11)(q24q14) associated with inversion, and the third, detected in a subclone, was described as der(11)(11pter->11q24::11q14->11q24::?). The most frequent additional

DOI: 10.1093/AJCP/AQX139

Table 1
Patient Characteristics

Patient No.	Age (y)/ Sex	Diagnosis	PS	CS	B	Bulky[a]	Site of Involvement	LDH > UNV	IPI	Treatment	Response	Status / Last FU (mo)
1	23/M	BLL,11q	0	II	No	No	T[b]	No	0	GMALL-B-ALL/ NHL2002	CR	ANED (50)
2	32/M	BLL,11q	1	II	No	No	T[b]	No	0	GMALL-B-ALL/ NHL2002	CR	ANED (38)
3	62/M	BLL,11q	1	IV	No	Yes[c]	LN/ab[d]	Yes	3	GMALL-B-ALL/ NHL2002	CR	ANED (43)
4	40/M	BLL,11q	1	IV	Yes	Yes[c]	LN/ab[b]	Yes	3	GMALL-B-ALL/ NHL2002	CR	ANED (56)
5	20/M	BLL,11q	4	IV	No	Yes[c]	LN/ab[b]	Yes	3	GMALL-B-ALL/ NHL2002	CR	TRM (1)
6	29/M	BLL,11q	0	I	No	No	LNc[d]	No	0	R-CODOX-M/R / R-IVAC, ESHAP	CR	ANED (67)
7	65/M	HGBL, NOS	2	IV	No	Yes	S/I/LN/ab[d]	No	1	DA-EPOCH-R, auto SCT	CR	ANED (10)
8	20/M	BL	1	II	No	No	LNc[b]	Yes	1	GMALL-B-ALL/ NHL2002	CR	ANED (98)
9	25/M	BL	0	I	No	No	T[b]	No	0	GMALL-B-ALL/ NHL2002	CR	ANED (71)
10	59/M	HGBL, NOS	1	IV	No	Yes	S/LN	Yes	1	R-CHOP GMALL-B-ALL/ NHL2002	PRpd	DOD (13)
11	41/M	BL[e]	0	I	No	Yes	LNab[b]	No	0	DA-EPOCH-R	CR	TUM (6)

ab, abdominal presentation of disease; ANED, alive, no evidence of disease; B, B symptoms; BLL,11q, Burkitt-like lymphoma with 11q aberration; BL, Burkitt lymphoma; c, cervical; CR, complete remission; CS, Ann Arbor Stage of disease; DA-EPOCH-R, dose-adjusted etoposide, prednisolone, vincristine, cyclophosphamide doxorubicin, and rituximab; DOD, died of disease progression; ESHAP, etoposide, methylprednisone, cytarabine, cysplatin; FU, follow-up (months after the final diagnosis or death); GMALL-B-ALL/NHL2002, rituximab, fractionated cyclophosphamide (or ifosfamide), vincristine, methotrexate, cytarabine, teniposide, and prednisone or doxorubicin; HGBL, NOS, high-grade B-cell lymphoma, not otherwise specified; I, intestine; IPI, International Prognostic Index score; IVAC, fractionated ifosfamide, etoposide, and high-dose cytarabine; LDH>UNV, lactate dehydrogenase elevated above the upper normal value; LN, lymph node; PRpd, partial remission followed by progression; PS, performance status; R, rituximab; R-CODOX-M/R-IVAC, fractionated cyclophosphamide, vincristine, doxorubicin, and high-dose methotrexate alternating with fractionated ifosfamide, etoposide, and high-dose cytarabine, along with intrathecal methotrexate and cytarabine; R-CHOP, rituximab, cyclophosphamide, doxorubicin, vincristine, and prednisone; S, stomach; T, tonsil; TRM, treatment-related mortality; TUM, treatment and disease unrelated mortality.
[a]Tumor >7 cm in the greatest dimension.
[b]One enlarged lymph node/tumor.
[c]Tumor >20 cm in the greatest dimension.
[d]A few/multiple enlarged lymph nodes/tumors.
[e]Patient 11 was HIV positive.

changes comprised 8q24/*MYC* translocations with *IGH*/14q32– or *IGL*/22q11 (patients 7-11), deletions of 6q (patients 1 and 2), and trisomy 12 (patients 3 and 6). Other chromosomal aberrations had random occurrence.

FISH Analysis of 11q-Gain/Loss Cases

All cases were analyzed by FISH with selected probes for 11q (Table 2). Aberrations of 11q were determined by ratio of the *CCND1*(11q13.3), *ATM*(11q22.3), *KMT2A*(11q23.3), and D11S1037(11q25) signals relative to signals of chromosome 11 centromeric probe (Figure 1). In patients 1 and 2, equal pattern of two signals of *CCND1*, *ATM*, and *KMT2A* on dup(11q) was observed. In patient 7, three signals of all three probes on aberrant chromosome 11 was detected indicating triplication of 11q. In five cases (patients 3-6 and 9), three to five copies of *KMT2A* relative to *CCND1* and/or *ATM* on aberrant chromosome 11 were observed, suggesting additional gain of this region. Patients 10 and 11 displayed two copies of *CCND1* and *ATM* and loss of the *KMT2A* signal on dup(11q). Reciprocal *CCND1*, *ATM*, and *KMT2A* signals position on aberrant chromosome 11 revealed inversion of the duplicated region (patients 1-4, 6-9, 10-11, respectively). In patient 9 and on one of the aberrant chromosome 11 in patient 6, dup(11q) was linear. In patient 5, inversion could not be assessed because the duplication was small—limited to the region covered only by KMT2A probe.

Telomeric losses of 11q were investigated using the D11S1037(11q25) probe. Loss of one D11S1037 signal in the presence of two centromeric signals was detected in 10 patients (1-5, 7-11). In the remaining case (patient 6), two or three signals of centromere 11 and two or three signals of D11S1037 were noticed.

Status of *MYC* was analyzed in all cases. Normal FISH pattern was detected in five patients (1-4 and 6). In patient 5 with trisomy 8, one additional copy of *MYC* was detected. All three *MYC* copies in this case were

DOI: 10.1093/AJCP/AQX139

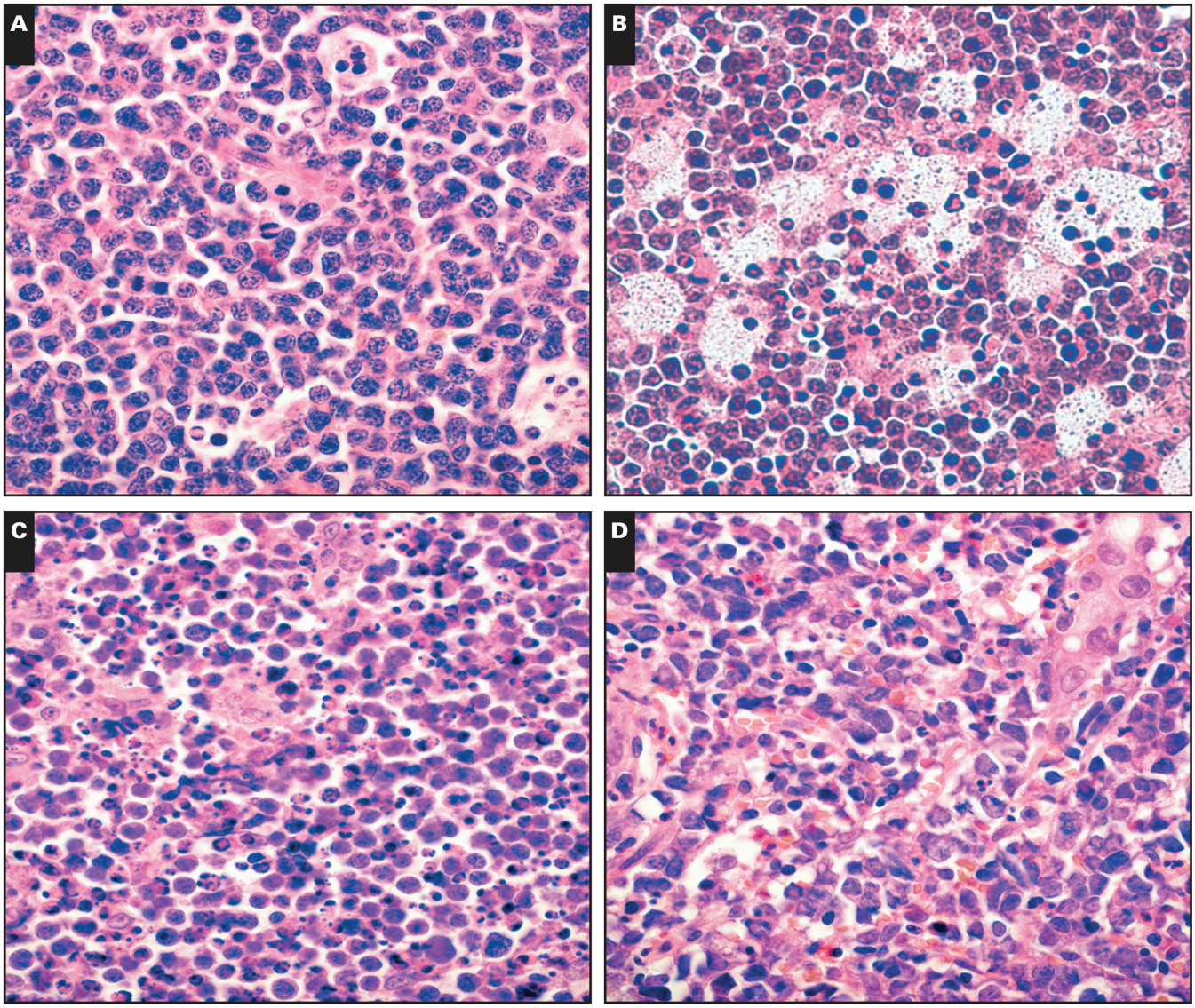

Image 1 Histopathologic features of patients 1 (**A**, tonsil) and 5 (**B**, abdominal lymph node) of Burkitt-like lymphoma with 11q aberration, patients 11 (**C**, axillary lymph node) and 7 (**D**, stomach) of Burkitt lymphoma (BL) and high-grade B-cell lymphomas, nototherwise specified (HGBL, NOS), respectively, carrying both *MYC* rearrangement and 11q aberration. Based on morphological assessment, these distinctions can be very subjective. Diffuse growth is composed of medium-sized lymphoid cells (**A**-**D**) showing jigsaw puzzle effect of cytoplasmic borders (**B**, **C**), with a starry-sky pattern due to admixed phagocytic macrophages (**A**-**C**). The nuclei are similar in size and shape (**A**-**C**), except for one case (**D**). H&E-stained sections show classic morphologic features of BL with a starry-sky pattern (**B**, **C**) and features slightly different from classic BL (**A**) by the reduced number of apoptotic bodies and reduced jigsaw puzzle effect, with the morphology of B-cell lymphoma, unclassifiable, with features intermediate between diffuse large B-cell lymphoma and BL. A case of HGBL, NOS, involving the stomach, makes morphological evaluation difficult. The architecture is diffusely effaced, cells appear more blastoid with mild degree of irregular nuclear contours, and there is no starry-sky pattern due to the lack of tingible-body macrophages (**D**) (paraffin section stained with H&E, ×600).

unrearranged. In five patients (7-11), harboring t(8q24), FISH detected rearrangement of *MYC*. We additionally analyzed the status of *BCL2* and *BCL6*. No structural changes of both genes were detected. Copy number gains and losses were observed sporadically and correlated with karyotypic changes (data not shown).

SNP/aCGH Analysis of Chromosome 11

SNP/aCGH was performed in all 11 patients and results of chromosome 11 profiling are summarized in Table 3 and illustrated in Figure 2 and Figure 3. Two main types of 11q rearrangements were detected—duplication of a big fragment of 11q (>50 Mbp) with accompanying terminal

DOI: 10.1093/AJCP/AQX139

Table 2
Results of Cytogenetic and FISH Analysis of the Reported Cases[a]

Type	Patient No.	Karyotype	FISH Signals on dup(11q)				
			11q13.3 *CCND1* Signals	11q22.3 *ATM* Signals	11q23.3 *KMT2A* Signals	11q25 D11S103 Signals	Inv of dup(11q)
MYC-negative	1	45,X,−Y,del(6)(q21),dup(11)(q24.3q12.1)[13]	2	2	2	0	+
	2	46,XY,?add(3)(q2?7),del(6)(q12q21),dup(11)(q24.1q13.1), der(18) t(3;18)(q2?7;q21)[12]	2	2	2	0	+
	3	46,XY,dup(11)(q23.3q22.2)[3]/47,sl,+12[7]/48,sdl1,+3[3]	1	2	3-5	0	+
	4	46,XY,dup(11)(q24.1q22.3)[11]	1	2	3-4	0	+
	5	47-48,XY,+8,dup(11)(q22.3q24.1),+1-4mar[cp7]/46XY[10]	1	1	3-5	0	?
	6	42-45,X,−Y[9],-4[4],add(4)(q12)[9],der(6)t(4;6)(q12;p25)[10], dup(11)(q14q24)[11],dup(11)(q24q14)[11], 1-2mar[8][cp11]/ 44-45,idem, der(11)(11pter->11q24::11q14->11q24::?)[cp6]	2	2-4	2-5	2-3	+
MYC-positive	7	45-47,XY,add(3)(q27)[8],+5[2],t(8;22)(q24;q11.2)[9],trp(11) (pter11->q23::q23->q13::q13->qter)[9],add(14)(q32)[3], −18[5],+mar1[2],+mar[2][cp9]	3	3	3	0	+
	8	46,XY,t(8;14)(q24;q32),dup(11)(q24.1q13.4)[1]/ 47,sl,+12[6]/47~48,sd1,+1-2mar[3]	1	2	2	0	+
	9	40-46,XY,t(8;14)(q24;q32)[8],dup(11)(q22.3q23.3)[8],der(13) (1q44→1q21::?11q13→?11q23::13p1?1)[5] [cp8]	1	2	2-3	0	–
	10	44-50,X-Y[4],dup(1)(q?21q23)[5],+7[2],t(8;14)(q24;q32)[5], dup(11)(q11q23)[5],add(16)(p13.3)[4],add(17)(p13)[4],+1mar [5][cp5]/46,XY[14]	2	2	0	0	+
	11	44-46,XY,add(3)(q2?9)[3],add(5)(p15)[4],t(8;22)(q24;q11)[10], dup(11)(q23q12)[10],add(13)(q22)[8],der(13)add(13)(p11.2), add(13)(q22)[2],add(18)(q21)[9],+mar[2][cp10]	2	2	0	0	+

FISH, fluorescence in situ hybridization; Inv, inversion—inversion could not be assessed by FISH probes, because of too small duplication region, smaller than distance between *ATM* and *KMT2A* probes.
[a]FISH results describe number of each probe signal on dup(11q) only. For detection accuracy, chromosome 11 centromeric probe was used. Except for patient 6, probe signals were related to one centromeric signal on dup(11q). In patient 6 with two or three dup(11) chromosomes, probe signals were related to two or three centromeric probes.

deletion (Figures 2 and 3A), and duplication of a small 11q region (<20 Mbp) with additional gain inside the duplicated region, also associated with a terminal deletion (Figures 2 and 3B). First type of duplication was noticed in six patients (1, 2, 7, 8, 10, 11). Duplicated regions ranged in size from 71.39 Mbp (11q12.1q24.3) to 51.27 Mbp (11q13.4q24.1). In case 11, additional gain in the duplication region was detected. The position of this change was 11q13.4q14.4 and different from additionally gained regions in the remaining cases. Size of the deleted terminal fragments ranged from 6.75 Mbp (11q24.3q25) to 21.09 Mbp (11q23.2q25). In the second type, smaller duplication was detected in four patients (3-5, 9). The duplication size ranged from 11.95 Mbp (11q22.3q24.1) to 18.97 Mbp (11q22.2q23.3). All four cases revealed additional gains within the duplicated regions, covering area of 1.46 Mbp to 5.26 Mbp. The smallest amplified region was detected in patient 3 and covered 48 genes, among others the *KMT2A* Table 4. Additional gains were constantly associated with the small 11q duplication ($P = .005$) and bulky tumor over 20 cm ($P = .033$). Deletion regions in these four cases extended from 11.36 Mbp (11q24.1q25) to 15.12 Mbp (11q23.3q25). In patient 4, additional biallelic deletion was detected. It covered a region of 774.52 kbp, which contains six genes: *ETS1*, *FLI1*, *KCNJ1*, *KCNJ5*, *C11orf45* and *TP53AIP1* (Table 4). Patient 6 carrying two or three dup(11q) does not fit into the two main groups because it is lacking the 11qter deletion. Instead, SNP distribution revealed an uniparental disomy (UPD) of 11q24.1q25, thus in the region commonly deleted in the other cases (Figure 3C). In patients 10 and 11, size of the terminal deletion was bigger than in all other cases: 21.09 Mbp (11q23.2q25) and 17.97 Mbp (11q23.3q25) respectively. In these cases, terminal deletions included *KMT2A*. In nine cases, simultaneous SNP analysis showed loss of heterozygosity (LOH) in the deleted 11q terminal region.

In summary, aCGH analysis did not detect conserved breakpoints of the gained and lost regions. The proximal breakpoints of duplication were scattered in the region of 53.5 Mbp (55,737,502-109,285,414) and distal breakpoints were scattered in the region of 14.4 Mbp (113,766,509-128,177,729). Considering breakpoints between gained and deleted regions, they ranged from 119,715,997 to 128,065,891 (8.3 Mbp). There was no gap between gain regions and terminal deletions—the distance between them ranged from 49 kbp to 165 kbp (average 92 kbp) and corresponded to the distance between two probes.

Discussion

Distinguishing BLL,11q from BL, including cases carrying both *MYC* rearrangement and 11q aberration,

DOI: 10.1093/AJCP/AQX139

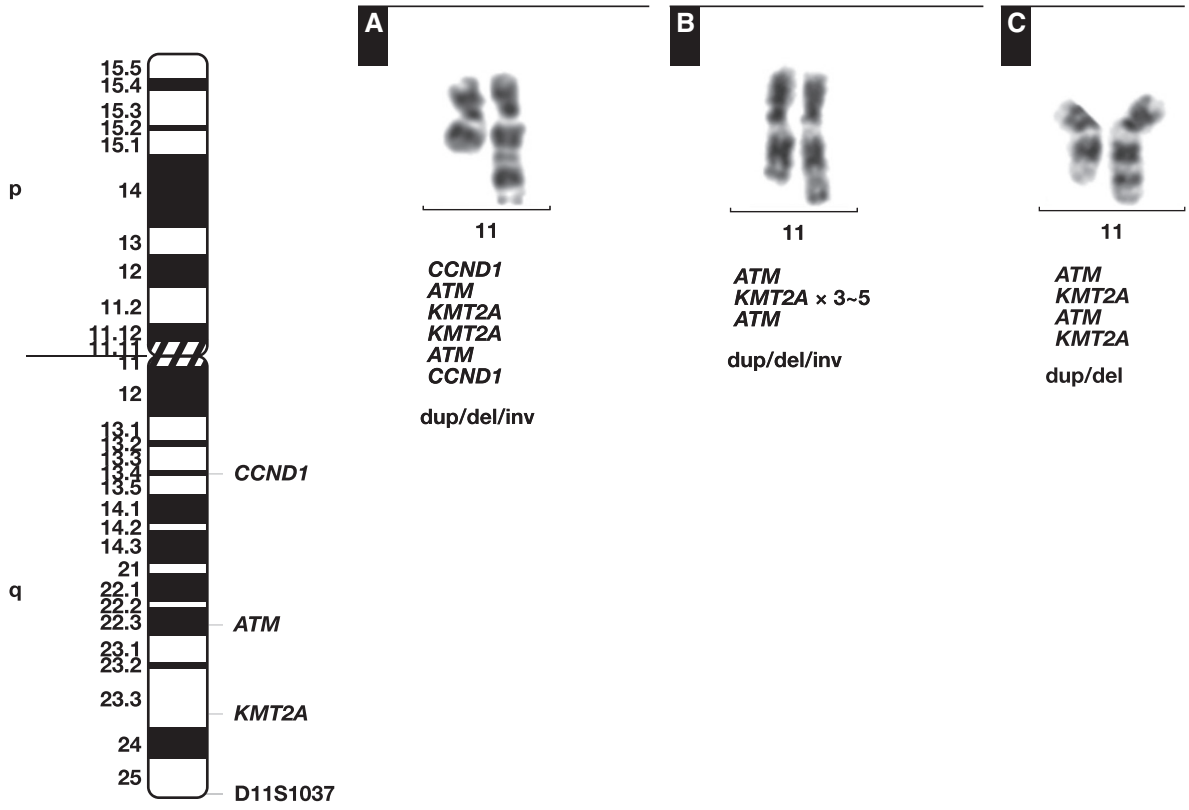

Figure 1 Different types of 11q aberrations in the reported cases. **A**, Big dup(11q) with inversion and terminal deletion. **B**, Small dup(11q) with inversion, additional internal gain, and terminal deletion. **C**, Small dup(11q) without inversion and with terminal deletion.

Table 3
Results of SNP/aCGH Analysis of Chromosome 11 in the Reported Cases[a]

Patient No.	CNV–11q Duplication	Size B/S[b]	CNV/SNP –11q Telomeric Losses or UDP	Size
MYC-negative				
1	11q12.1q24.3 (56,790,631-128,177,729) x3	71.39 Mbp B	11q24.3q25 (128,177,670-134,931,948) x1	6.75 Mbp
2	11q13.1q24.1 (64,392,013-121,599,032) x3	57.21 Mbp B	11q24.1q25 (121,529,800-134,931,948) x1	13.4 Mbp
3	11q22.2q23.3 (102,144,117-121,118,244) x3	18.97 Mbp S	11q24.1q25 (121,346,328-134,931,948) x1	13.59 Mbp
	11q23.3 (117,815,640-119,275,901) x4	**1.46 Mbp**		
4	11q22.3q24.1 (106,120,397-123,495,005) x3	17.37 Mbp S	11q24.1q25 (123,572,602-134,931,948) x1	11.36 Mbp
	11q23.3q24.1 (118,239,916-123,495,005) x4	**5.26 Mbp**	**11q24.3 (128,039,399-128,813,918) x0**	**774.52 kbp**
5	11q22.3q24.1 (109,285,414-121,236,822) x5	11.95 Mbp S	11q24.1q25 (121,302,822-134,931,948) x1	13.63 Mbp
	11q23.3 (116,612,808-118,689,296) x7	**2.08 Mbp**		
6	11q14.1q24.1 (80,201,232-121,236,822) x3	41.04 Mbp ?	*11q24.1q25(121,335,329-134,586,308)*	*13.25 Mbp*
	11q22.3q23.3 (107,196,633-120,744,339) x3	**13.55 Mbp**		
MYC-positive				
7	11q13.1q24.2 (65,422,918-124,646,116) x3	59.22 Mbp B	11q24.2q25 (124,730,404-134,931,948)x1	10.2 Mbp
8	11q13.4q24.1 (72,148,579-123,414,746) x3	51.27 Mbp B	11q24.1q25 (123,572,602-134,931,948) x1	11.36 Mbp
9	11q22.3q23.3 (105,344,712-119,715,997) x3	14.37 Mbp S	11q23.3q25 (119,807,473-134,931,948) x1	15.12 Mbp
	11q23.3 (116,723,888-119,715,997) x5	**2.99 Mbp**		
10	11q13.1q23.3 (64,805,605-116,874,857) x3	52.07 Mbp B	11q23.3q25 (116,961,138-134,931,948)x1	17.97 Mbp
11	11q12.1q23.2 (55,737,502-113,766,509) x3	58.03 Mbp B	11q23.2q25 (113,843,488-134,931,948)x1	21.09 Mbp
	11q13.4q14.3(73,706,649-89,344,089) x4	**15.64 Mbp**		

aCGH, array-based comparative genomic hybridization; bp, base pair; CNV, copy number variation; SNP, single nucleotide polymorphism; UDP, uniparental disomy.
[a]Bold font indicates regions of additional gains in regions of dup(11q) and the region of biallelic deletion. Italic font shows UPD region without terminal deletion.
[b]Category of size duplicated region: B, big, >50 Mbp; S, small, <20 Mbp; ?, outsized duplication and additional gain regions caused by the presence of two or three aberrant chromosomes with 11q-gain/loss.

and *MYC*-positive HGBL, NOS, based on the morphologic and immunohistochemical criteria is difficult, even for expert hematopathologists. Due to overlapping pathomorphological features of the above-mentioned entities/categories, following preliminary morphological diagnosis of "aggressive B-cell lymphomas resembling BL," these cases always require further molecular and cytogenetics detailed diagnostics.

DOI: 10.1093/AJCP/AQX139

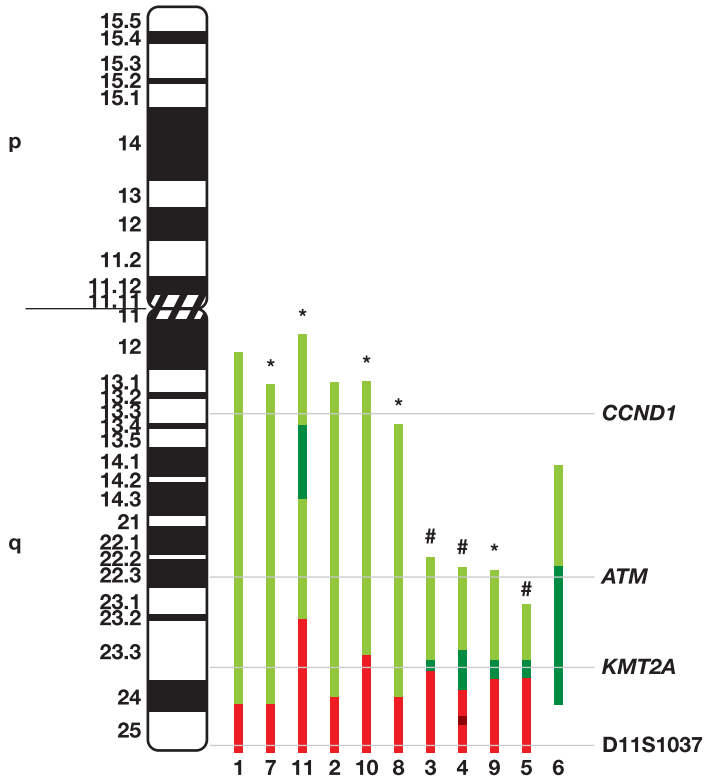

Figure 2 Summarized results of chromosome 11 profiling by single nucleotide polymorphism/array-based comparative genomic hybridization. Duplicated regions are depicted in light green—additional gains in the duplicated regions are shown in dark green. Red color indicates terminal 11q deletion regions. The brown spot in patient 4 marks a biallelic deletion. Patient numbers are indicated in the bottom of the graph. The patients are ordered according to the size of the duplication. *Indicates *MYC*-positive cases. #Indicates cases with tumor size more than 20 cm.

The 11 reported here—new B-NHL cases with the recently described 11q-gain/loss aberration[1–3]—were documented by conventional and molecular cytogenetics. All cases revealed a duplication of 11q, which in all but 1 case was inverted. Duplicated regions varied in size, revealing 2 types of duplication size bigger (>50 Mbp) and smaller (<20 Mbp), with the smallest duplicated region determined by SNP/aCGH, which covered approximately 12 Mbp. Of interest, the small duplication was usually associated with additional gain of the region, including *KMT2A*. Presumably this region contains targeted amplified genes. It is worth noting that presence of additional gains in the duplicated region coincides with bulky tumor with dimension over 20 cm, found mainly in the retroperitoneum, suggesting association of amp(11q) with the progression of the disease.

SNP/aCGH analysis allowed to define the minimal duplication region (MDR) of 11.95 Mbp and the minimal gained region (MGR) of 1.46 Mbp, which were mapped at 11q22.3q24.1 (Chr11: 109,285,414-121,236,822) and 11q23.3 (Chr11: 117,815,640-119,275,901), respectively. Comparison of our data with findings of Salaverria et al[2] and Ferreiro et al[3] is shown in Table 4. In our series, MDR was much larger than described by both groups, but comprised the candidate *PAFAH1B2*, *USP2*, and *CBL* oncogenes.[2,3] The MGR was larger than the amplified region detected by Salaverria et al,[2] but both regions were overlapping. Given that *KMT2A* frequently included in the amplified region was affected by a terminal deletion in two cases, we excluded this gene as a candidate target of the 11q gain.

The proximal and distal breakpoints of the 11q gain were not specific as in the cases analyzed by Salaverria et al.[2]

Terminal 11q losses were detected in 10 out of 11 cases. The size of deleted region varied, but the minimal lost region (MLR) of 6.75 Mbp was mapped at 11q24.4q25 (Chr11: 128,177,670-134,931,948). The MLR size was similar to MLR described by Salaverria et al[2] (7.4 Mbp) (Ch11: 127,471,805-134,940,727), but smaller than observed by Ferreiro et al[3] (13.5 Mbp) (Chr11: 121,499,571-135,006,516). In one case, a focal biallelic deletion of 774 kbp mapped at 11q24.3

DOI: 10.1093/AJCP/AQX139

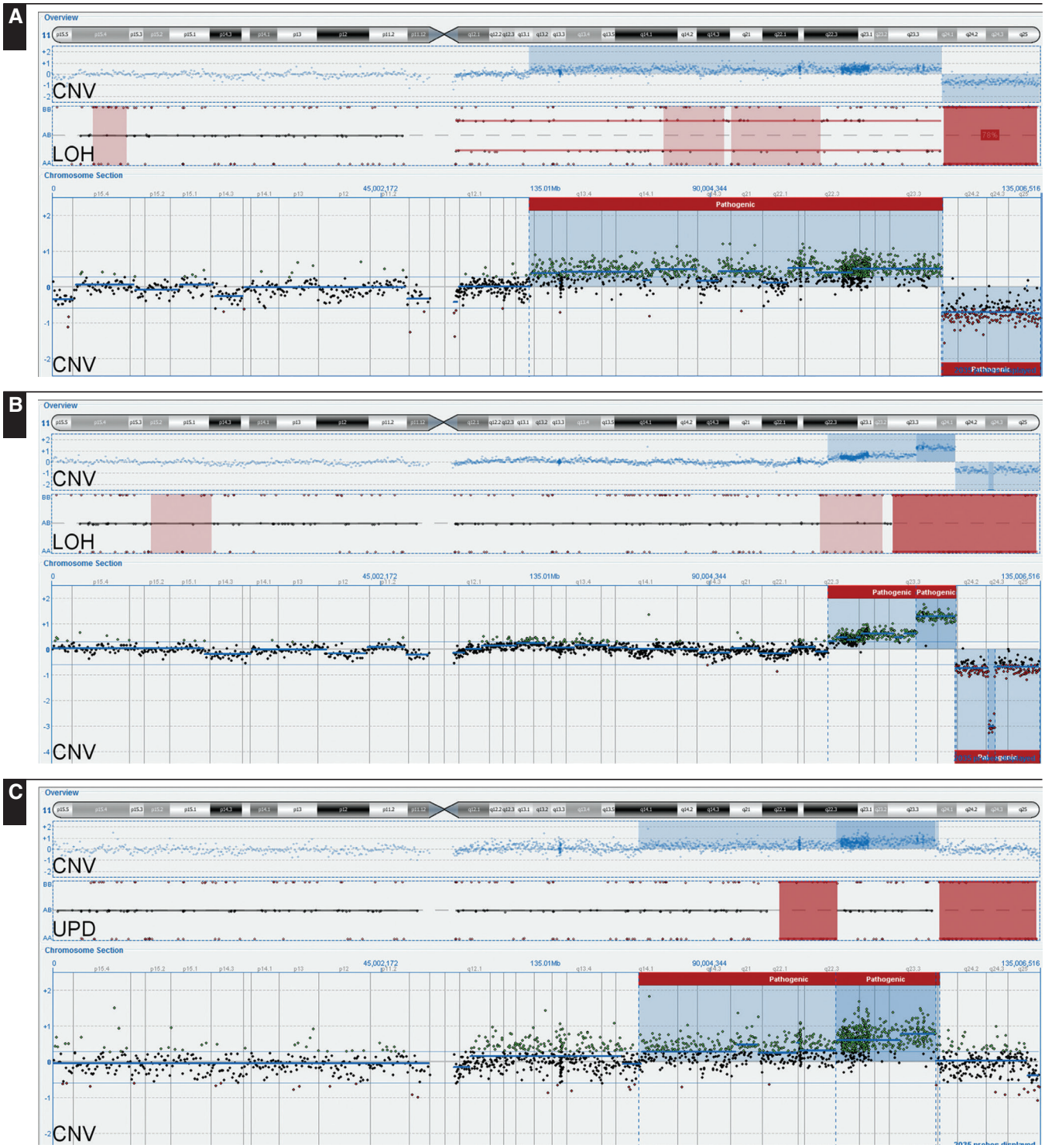

Figure 3 Results of chromosome 11 profiling by single nucleotide polymorphism/array-based comparative genomic hybridization (SNP/aCGH) in three patients: 2 (**A**), 4 (**B**), and 6 (**C**). The overview window shows ideogram of chromosome 11, below result of SNP/aCGH as a copy number variations (CNV) indicating duplication, additional gains and deletion of 11q, underneath big red blocks demonstrating loss of heterozygosity (LOH) or uniparental disomy (UPD) regions revealed in SNP analysis. Lower section shows magnification of a CGH analysis (CNV). Green dots indicate gain; red dots shows deletion regions. **A** is an example of bigger 11q duplication region and terminal deletion. **B** shows 11q duplication, with additional gain region and terminal deletion with small (774.52 kilobase pairs) homozygous deletion. **C** indicates 11q duplication with multiplication region without terminal deletion. In SNP analysis, the first dark red block indicates UPD in a fragment of duplication region; the second shows terminal LOH without CNV that indicates UPD, which corresponds to the deletion region in other cases.

DOI: 10.1093/AJCP/AQX139

(Ch11: 128,039,399-128,813,918) and comprising *ETS1*, *FLI1*, *KCNJ1*, *KCNJ5*, *C11orf45*, and *TP53AIP1* was detected. The deleted region overlapped with the biallelic deletion described by Salaverria et al[2] (1.5 Mbp). Our findings confirm a possible role of *FLI1* and *ETS1* in pathogenesis of these tumors, as previously suggested.[2] *FLI1* and *ETS1* have already been shown to be involved in hematologic neoplasms, including lymphomas.[10-13]

Interestingly, one patient with dup(11q) showed lack of 11q terminal deletion. Nevertheless this patient was included in the investigated group, since it revealed the presence of UPD in the terminal 11q region. We were able to detect UPD of 11q owing to simultaneous use of SNPs on the CGH array. UPD is a mechanism used to eliminate one copy of the DNA fragment and replacing it with the remaining copy, usually with mutation or to uncover recessive genes. Acquired UPD is quite common in both hematologic and solid tumors, and reported to constitute 20% to 80% of the LOH seen in human tumors.[14-17] We presume that in 11q deleted region suppressor gene(s) are present, which inactivation can promote tumorigenesis of 11q-gain/loss cases. The UPD mechanism could have eliminated a wild copy of tumor suppressor gene and replaced by mutated copy. An example can be *ETS1*, which mutations and biallelic deletion were revealed by Salaverria et al[2] in patients with 11q-gain/loss. Another possible consequence of UPD is different imprinting of gene allele promotors that are differentially silenced and deletion can lead either to gain or loss of imprinting. This can result in changes in gene expression similar to the effect of deletion. In a situation where the transcription of both alleles is essential for normal cell functioning, deletion and sequence replacing by another gene copy can play pathogenic role.[17]

Our SNP/aCGH analysis showed LOH in 11q terminal deletion region in all but one case. In this case, LOH was not noticed despite the presence of 11q terminal deletion in the CNV analysis. The absence of LOH was most likely related to the size of the deletion (6.75 Mbp), lower than the SNP resolution.

Of note, all our cases with 11q-gain/loss but one presented inversion of the duplicated 11q region, like in several previously reported cases.[1,3] This peculiar pattern of aberrations was identified in some cases in constitutional cytogenetics. Inversion, duplication, and terminal deletion has been described for many chromosomes 2q,4p,5p,7q,9p,13q and 18q.[18] This type of aberration, except for 11q-gain/loss, has not been described in hematologic malignancies. It remains unresolved whether or how inversion plays a role in activation of oncogenes in lymphoma cases with 11q-gain/loss.

The most intriguing in our finding was detection of 11q-gain/loss in five *MYC*-positive lymphoma cases. This finding was preliminarily published, describing cytogenetic data of four out of five cases presented in this article.[19] Simultaneous presence of these two aberrations indicate that 11q-gain/loss is not specifically associated with *MYC*-negative BLL,11q, but may be present also in the classic BL and HGBL, NOS, with *MYC* rearrangement. Our results are in accordance with recently published data. Havelange et al[6] described one case of *MYC*-positive lymphoma with 11q-gain/loss.

Based on the data available so far, it is unclear whether 11q-gain/loss is a primary or secondary hit in the *MYC*-positive BL and HGBL, NOS. These cases were characterized by a higher number of aberrations in comparison with *MYC*-negative cases with 11q-gain/loss (average, 6.4 vs 4.3). Interestingly, recent data suggest that *MYC* translocation is insufficient to cause BL.[20] It has been speculated that other genomic changes, like mutations of *TCF3*, *ID3*, and *CCND3*, are necessary to cause overt BL phenotype. We hypothesize that the 11q-gain/loss aberration, which seems to replace t(8q24) in *MYC*-negative lymphomas, may enhance effect of t(8q24) and codrives pathogenesis of *MYC*-positive lymphomas.

Recognition of the new BLL,11q entity leads to necessity of detection of 11q aberrations. For fast analysis, the basic panel of three probes consisting of CEP11, KMT2A, and tel 11q can be used. Number of *KMT2A* and tel 11q signals in relation to CEP11 can show 11q duplication type. *KMT2A* duplication with tel 11q deletion indicates bigger duplication and additional gain of *KMT2A* with tel 11q deletion defines smaller duplication. This test can be performed on fresh material, as well as on paraffin sections. In case of ambiguous results, like big 11q deletion, including *KMT2A*, for accurate detection of 11q-gain/loss, we propose extended panel of five probes: CEP11, CCND1, ATM, KMT2A, and tel 11q and, as far as possible, analysis of the hybridization result on metaphases. This approach can define duplication, internal 11q multiplication, inversion, and deletion pattern. These two FISH strategies can be especially useful in the choice of therapy in ambiguous cases with BL characteristic and lack of *MYC* rearrangement.

Conclusions

We have characterized 11q-gain/loss aberration in 11 patients with diagnoses BLL,11q, BL, and HGBL, NOS. The gain of 11q was accompanied by inversion of dup(11q) in most cases. Two types of duplication were detected—bigger than 50 Mbp and smaller than 20 Mbp—with internal amplification containing *KMT2A*, which was associated with bulky tumor over 20 cm in diameter. There were no conservative breakpoints on 11q. Terminal deletions were different sizes. The UPD of 11q found in one case seems to replace del(11q) probably by the loss of gene functions located in this region. One case showed a focal biallelic

DOI: 10.1093/AJCP/AQX139

Table 4
Changes of 11q Detected by Array-Based Comparative Genomic Hybridization[a]

hg19	Our Results	Salaverria et al[2]	Ferreiro et al[3]
Minimal 11q duplication region			
Duplication size	11.95 Mbp	3.4 Mbp	4 Mbp
Position on chromosome 11	Chr11: 109,285,414-121,236,822	Chr11: 115,025,608-118,434,149	Chr11: 116,072,765-120,087,526
Minimal gained region (MGR) region size	1.46 Mbp	0.832 Mbp	—
Position on chromosome 11	Chr11: 117,815,640-119,275,901	Chr11: 117,602,151-118,434,149	—
Genes	***IL10RA; TMPRSS4; SCN4B; SCN2B; AMICA1; MPZL3; MPZL2; CD3E; CD3D; CD3G; UBE4A; ATP5L; KMT2A; TTC36; TMEM25; IFT46; ARCN1***; *PHLDB1; TREH; DDX6; CXCR5; BCL9L; MIR4492; UPK2; FOXR1; CCDC84; RPS25; TRAPPC4; MIR3656; SLC37A4; HYOU1; VPS11; HMBS; H2AFX; DPAGT1; C2CD2L; HINFP; ABCG4; NLRX1; PDZD3; CCDC153; CBL; MCAM; RNF26; MFRP; C1QTNF5; MFRP; USP2*	*DSCAML1; FXYD2; FXYD6; TMPRSS13;* ***IL10RA; TMPRSS4; SCN4B; SCN2B; AMICA1; MPZL3; MPZL2; CD3E; CD3D; CD3G; UBE4A; ATP5L; KMT2A; TTC36; TMEM25; IFT46; ARCN1***	Not indicated
Minimal 11q deletion region			
Deletion size	6.75 Mbp	7.4 Mbp	13.5 Mbp
Position on chromosome 11	Chr11: 128,177,670-134,931,948	Ch11:127,471,805-134,940,727	Chr11:121,499,571-135,006,516
Biallelic deletion	0.774 Mbp	1.5 Mbp	Not detected
Position on chromosome 11	Chr11:128,039,399-128,813,918	Chr11:127,816,801-129,341,359	
Genes	***ETS1; FLI1; KCNJ1; KCNJ5; C11orf45; TP53AIP1***	***ETS1; FLI1; KCNJ1; KCNJ5; C11orf45; TP53AIP1***; *RICS; BARX2*	

bp, base pair.
[a]All chromosome positions are given by hq19. Bold font indicates overlapping genes in minimal gained region and biallelic deletion region detected in presented work and published by Salaverria et al.

homozygous deletion among others, comprising two transcription factors, *FLI1* and *ETS1*. These observations suggest that in the described cases dose of genes—both gains and losses—are more important than their juxtaposition. Our study confirmed that 11q-gain/loss is a distinctive feature for *MYC*-negative BLL,11q. However, we have shown that this aberration is not specific for this subgroup. The 11q-gain/loss also occurs recurrently in *MYC*-positive BL and *MYC*-positive HGBL, NOS. This novel finding indicates that 11q aberration can be a primary or a secondary genetic change in the development of aggressive B-NHL.

Corresponding author: Beata Grygalewicz, PhD, Cytogenetic Laboratory, Maria Sklodowska-Curie Institute-Oncology Center, Warsaw, Poland, 15B Wawelska St, 02-034 Warsaw, Poland; bgrygal@coi.pl.

Acknowledgments: The authors thank Wojciech Michalski for his valuable help with statistical analyses, and Magdalena Bartnik, Barbara Wisniowiecka, and Marta Kedzior for technical assistance in carrying out SNP/CGH arrays procedure.

All array data are available from the GEO accession number GSE98371.

References

1. Pienkowska-Grela B, Rymkiewicz G, Grygalewicz B, et al. Partial trisomy 11, dup(11)(q23q13), as a defect characterizing lymphomas with Burkitt pathomorphology without MYC gene rearrangement. *Med Oncol*. 2011;28:1589-1595.
2. Salaverria I, Martin-Guerrero I, Wagener R, et al. Molecular Mechanisms in Malignant Lymphoma Network Project; Berlin-Frankfurt-Münster Non-Hodgkin Lymphoma Group. A recurrent 11q aberration pattern characterizes a subset of MYC-negative high-grade B-cell lymphomas resembling Burkitt lymphoma. *Blood*. 2014;123:1187-1198.
3. Ferreiro JF, Morscio J, Dierickx D, et al. Post-transplant molecularly defined Burkitt lymphomas are frequently MYC-negative and characterized by the 11q-gain/loss pattern. *Haematologica*. 2015;100:e275-e279.
4. Swerdlow SH, Campo E, Pileri SA, et al. The 2016 revision of the World Health Organization classification of lymphoid neoplasms. *Blood*. 2016;127:2375-2390.
5. Zajdel M, Rymkiewicz G, Chechlinska M, et al. miR expression in MYC-negative DLBCL/BL with partial trisomy 11 is similar to classical Burkitt lymphoma and different from diffuse large B-cell lymphoma. *Tumour Biol*. 2015;36:5377-5388.

DOI: 10.1093/AJCP/AQX139

6. Havelange V, Ameye G, Théate I, et al. The peculiar 11q-gain/loss aberration reported in a subset of MYC-negative high-grade B-cell lymphomas can also occur in a MYC-rearranged lymphoma. *Cancer Genet*. 2016;209:117-118.
7. McGowan-Jordan J, Simons A, Schmid M, eds. *ISCN 2016: An International System for Human Cytogenetic Nomenclature*. New York: Karger; 2016.
8. Grygalewicz B, Woroniecka R, Rygier J, et al. Monoallelic and biallelic deletions of 13q14 in a group of CLL/SLL patients investigated by CGH Haematological Cancer and SNP array (8x60k). *Mol Cytogenet*. 2016;9:1.
9. Sund KL, Zimmerman SL, Thomas C, et al. Regions of homozygosity identified by SNP microarray analysis aid in the diagnosis of autosomal recessive disease and incidentally detect parental blood relationships. *Genet Med*. 2013;15:70-78.
10. Zhang XK, Moussa O, LaRue A, et al. The transcription factor Fli-1 modulates marginal zone and follicular B-cell development in mice. *J Immunol*. 2008;181:1644-1654.
11. Morin RD, Mendez-Lago M, Mungall AJ, et al. Frequent mutation of histone-modifying genes in non-Hodgkin lymphoma. *Nature*. 2011;476:298-303.
12. Testoni M, Chung EY, Priebe V, et al. The transcription factor ETS1 in lymphomas: friend or foe? *Leuk Lymphoma*. 2015;56:1975-1980.
13. Bonetti P, Testoni M, Scandurra M, et al. Deregulation of *ETS1* and *FLI1* contributes to the pathogenesis of diffuse large B-cell lymphoma. *Blood*. 2013;122:2233-2241.
14. Nielaender I, Martín-Subero JI, Wagner F, et al. Partial uniparental disomy: a recurrent genetic mechanism alternative to chromosomal deletion in malignant lymphoma. *Leukemia*. 2006;20:904-905.
15. Gondek LP, Tiu R, O'Keefe CL, et al. Chromosomal lesions and uniparental disomy detected by SNP arrays in MDS, MDS/MPD, and MDS-derived AML. *Blood*. 2008;111:1534-1542.
16. O'Shea D, O'Riain C, Gupta M, et al. Regions of acquired uniparental disomy at diagnosis of follicular lymphoma are associated with both overall survival and risk of transformation. *Blood*. 2009;113:2298-2301.
17. Makishima H, Maciejewski JP. Pathogenesis and consequences of uniparental disomy in cancer. *Clin Cancer Res*. 2011;17:3913-3923.
18. Hermetz KE, Newman S, Conneely KN, et al. Large inverted duplications in the human genome form via a fold-back mechanism. *Plos Genet*. 2014;10:e1004139.
19. Rymkiewicz G, Chechlinska M, Grygalewicz B, et al. Significance of a critical set of 11q chromosome aberrations for diagnosis of MYC-negative Burkitt lymphoma. Presented at the 57th annual meeting of the American Society of Hematology; December 2015; Orlando, FL. Poster 2679. https://ash.confex.com/ash/2015/webprogramscheduler/Paper84544.html. Accessed May 26, 2017.
20. Schmitz R, Young RM, Ceribelli M, et al. Burkitt lymphoma pathogenesis and therapeutic targets from structural and functional genomics. *Nature*. 2012;490:116-120.

DOI: 10.1093/AJCP/AQX139

HOLOGIC®

First and Only FDA Cleared
Digital Cytology System

Genius™ Cervical AI

Genius™ Review Station

Genius™ Digital Imager

Empower Your Genius With Ours

Make a Greater Impact on Cervical Cancer
with the Advanced Technology of the
Genius™ Digital Diagnostics System

Click or Scan
to discover more

genius™
DIGITAL DIAGNOSTICS